Experimental report

29/09/2023

Proposal: 8-02-994 **Council:** 10/2022

Title: Phospholipid bilayer of pulmonary surfactant: the effect of lipopolysaccharide and Polymyxin B - II.

Research area: Other...

This proposal is a continuation of 8-02-927

Main proposer: Daniela UHRIKOVA

Experimental team: Daniela UHRIKOVA
Norbert KUCERKA
Lukas HUBCIK

Local contacts: Bruno DEME

Samples: DPPC/POPC/PLPC/POPG
DPPC/POPC/PLPC/POPG + PxB
DPPC/POPC/PLPC/POPG/LPS + PxB
DPPC/POPC/PLPC/POPG+LPS

Instrument	Requested days	Allocated days	From	To
D16	7	7	15/05/2023	22/05/2023

Abstract:

Bacterial lipopolysaccharide (LPS) can interfere with a pulmonary surfactant (PS), a mixture of phospholipids and specific proteins that decreases surface tension at the air¿liquid interface of lung¿s alveoli. LPS disturbs the function and structure of PS. Polymyxin B (PxB), a peptide based antibiotic, acts as an inhibitor of these changes. Oriented lipid bilayers deposited on silicon wafers and hydrated from vapour mimic well the PS lamellar structures. We performed a SAND experiment at D16 (Exp 802927) to examine structural changes of the PS model system infected by LPS and healed by PxB. Samples were hydrated by 8 % D2O showing the scattering from membranes only (water molecules being invisible). Reconstructed NSLD profiles of the bilayers indicate difference in PxB binding at lipid-water interface of PS+LPS depending on LPS content. We propose further study of the system hydrated with D2O/H2O mixtures varying the contrast between the lipid bilayers and water. The lipid bilayer thickness, the water distribution profile and the width of the bilayer ¿ water interface obtained from reconstructed NSLD profiles will elucidate the PxB binding. Experiments are related to in vivo study.

Experimental Report

Experiment title: Phospholipid bilayer of pulmonary surfactant: the effect of lipopolysaccharide and Polymyxin B – continuation

Proposers/participants: D. Uhríková[1*], N. Kučerka[1], L. Hubčík[1], B. Demé[2]
[1] Faculty of Pharmacy, Comenius University Bratislava, Slovakia
[2] ILL, Grenoble, France
Email*: uhrikova@fpharm.uniba.sk

Abstract:
Bacterial lipopolysaccharide (LPS) can interfere with a pulmonary surfactant (PS), a mixture of phospholipids and specific proteins that decreases surface tension at the air–liquid interface of the lung alveoli. LPS alters the function and structure of PS. Polymyxin B (PxB), a peptide based antibiotic, acts as an inhibitor of these changes. Oriented lipid bilayers deposited on silicon wafers and hydrated from vapour mimic well the PS lamellar structures. We performed a SAND experiment at D16 (Exp 802927) to examine structural changes in the PS model system infected by LPS and healed by PxB. Samples were hydrated with 8 % D_2O (D_2O/H_2O mixture) showing the scattering from the membranes only (water molecules are invisible). Reconstructed NSLD profiles of the bilayers indicate a difference in the binding of PxB at the lipid-water interface of PS+LPS, depending on the LPS content. The thickness of the lipid bilayer, the water distribution profile and the width of the bilayer – water interface obtained from reconstructed NSLD profiles obtained from 4 contrasts will elucidate the binding of PxB. Experiments are related to an *in vivo* study.

Background:
After inhalation, bacterial lipopolysaccharide (LPS) molecules interfere with a pulmonary surfactant (PS, Fig. 1a), a unique mixture of phospholipids and specific proteins (< 10 %) that decreases surface tension at the air-liquid interface of lung alveoli. The infection can be treated by exogenous PS administered intratracheally to premature babies and ventilated Covid-19 patients if necessary. LPS incorporated into clinically used exogenous porcine surfactant prevents the PS from reaching the necessary low tension during area compression and disturbs its lamellar structures in the water phase by swelling, as documented by our SAXS experiments [1]. Polymyxin B (PxB), a cationic peptide antibiotic, acts as an inhibitor of these structural changes [1]. We performed a neutron diffraction experiment at D16 beamline to determine structural parameters of synthetic pulmonary surfactant (MPS) composed of DPPC/POPC/PLPC/POPG and LPS, interacting with PxB. The prepared lipid dispersions were deposited on silicon wafers. Samples were hydrated in vapour of 8% D_2O that has a net zero coherent neutron scattering length density (NSLD) and the bilayer structure is not obscured by scattering from the solvent. High-quality oriented stacks were confirmed by observing up to 5 orders of diffraction peaks; an example of rocking curves is shown in the Experimental report [2].

We have found: Fig. 1b shows the extracted repeat distances as a function of hydration (% RH) for the MPS system and the surfactant infected by LPS. The repeat distance d increases nonlinearly with increasing hydration characterized by RH (%), and with the content of LPS. As a result of hydrophobic interactions between LPS acyl chains of lipid A and hydrophobic core of PS, LPS intercalates into the PS bilayer. $d=d_w+d_B$, and both parts, the lipid bilayer thickness (d_B) and the thickness of the water layer (d_w) can be affected. Fig. 1c shows an example of reconstructed NSLD of the lipid bilayer. The two maxima correspond to the head-to-head distance across the bilayer, d_{HH}. It is a parameter related to the thickness of the lipid bilayer (d_B). Data analysis has shown that d_{HH} increases slightly with the increasing LPS content in the bilayer (Fig. 1d). PxB slightly decreases the d_{HH} of MPS (Fig. 1d, gray square). Interestingly, 4wt% of PxB added to MPS+5% LPS does not affect d_{HH} when compared with MPS+5 % LPS itself (Fig. 1d, red square). The green curve in Fig. 1e results from the subtraction of the two NSLD profiles: (MPS+5%LPS+4%PxB)-(MPS+5%LPS), and can be attributed to the NSLD of PxB localized in the polar region of the bilayer. The difference in the repeat distances (d) of the two systems indicates that PxB exerts its activity through electrostatic interactions [Fig. 4B in 2]. However, at higher LPS content (10 wt%), we found different values of d_{HH} for the two systems, MPS+10%LPS+4%PxB and MPS+10%LPS (Fig. 1d, blue square). The results obtained indicate a difference in the localization of PxB in dependence on the content of LPS.

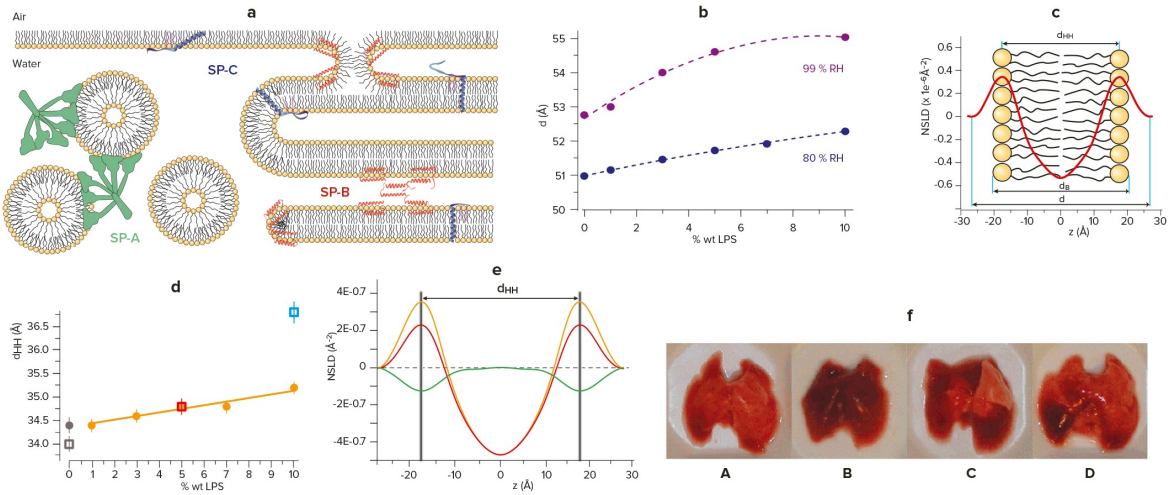

Fig. 1. a) Sketch of pulmonary surfactant structure; b) Repeat distances (d) as a function of the LPS content in two RH (%); c) NSLD profile of MPS (99 % RH); d) d_{HH} as a function of the LPS content (solid points) and the effect of PxB (open squares); e) NSLD profiles of MPS+5%LPS+4%PxB (red), MPS+5%LPS (yellow) and PxB (green); f) The lungs of preterm newborn rabbits after administration of: A- saline and exogenous surfactant; B- LPS only; C- LPS and surfactant; D- LPS and surfactant with 3 wt% PxB [3].

The analysis of data has shown the need to extend the measurement ([2] - ILL Experimental report 8-02-927, 2021). Further measurements for samples hydrated with different D_2O/H_2O mixtures vary the contrast between the lipid bilayers and water without changing the structure of lipid bilayers themselves. Analysis of such data allows for a model-free reconstruction of NSLD profiles that otherwise appears highly nontrivial in the case of systems with the complex composition. The reconstructed NSLD profiles then give the water distribution profile, the lipid bilayer thickness (d_B), and the width of the bilayer – water interface [4].

Experiment:

The phospholipids were purchased from Avanti Polar Lipids (Alabaster, AL) and used without further purification. Mixtures of MPS and LPS were prepared as follow [5]. Approximately 12 mg of lipid mixture (thin film composed of 2,000-3,000 bilayers having a total thickness ~15 μm when spread over a 25 x 50 mm^2 silicon wafer) was hydrated with deionized water and thoroughly mixed, several freeze-thaw cycles was applied and vortexing vigorously. MPS+LPS was incubated with PxB prior to dispersion deposition. The dispersions were deposited on leveled silicon wafers that were heated to 50 °C, and excess water was left to evaporate. Care was taken to form lipid multilayers in the fluid phase and to anneal the samples for several hours upon rehydration. The samples were hydrated in the vapour of 4 mixtures of D_2O/H_2O at constant humidity according to [4], using an airtight hydration chamber provided by ILL. High-quality oriented stacks were confirmed by observing up to 5 orders of diffraction peaks; an example of rocking curves is shown in Fig. 2.

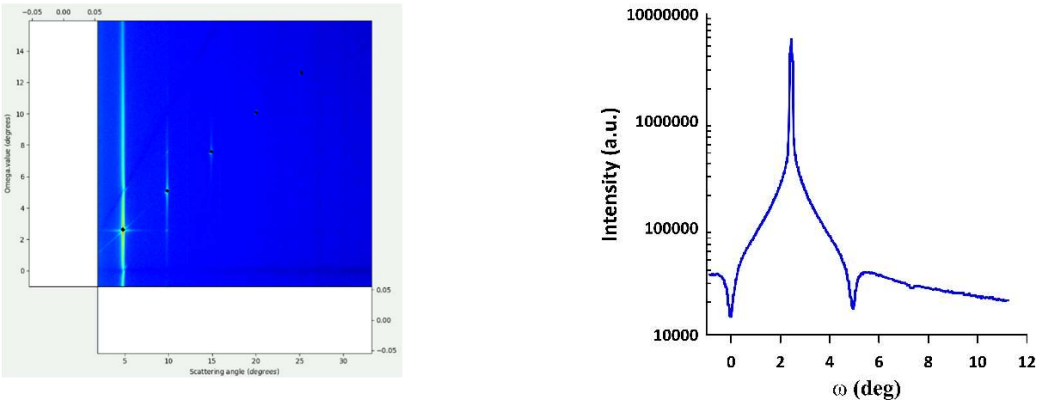

Fig. 2. 2D image of a SAND measurement. The rocking curve of the first peak of the MPS+3 wt% LPS+4 wt% PxB sample. FWHM ~ 0.05° obtained from the combined Gaussian/Lorentzian fit confirms the well-oriented sample [4 and therein].

Small-Angle Neutron Diffraction

Neutron diffraction data were collected at the Institut Laue-Langevin (ILL) in Grenoble, France, on a D16 small momentum transfer diffractometer with variable vertical focusing. Neutrons of 4.503 Å wavelength were selected by

(002) reflection of a pyrolytic graphite (PG) monochromator. The incoming beam was formed by the set of slits (S1=150x6 mm^2 and S2=30x5 mm^2) and the sample-to-detector distance was 1.16 m. All samples were measured at one detector position, with a scan $-1^o \leq \Omega \leq 16^o$ with step 0.05^o and acquisition 15 s. Area detector data were visualized and reduced using the Mantid software provided by ILL [6].

Results and discussion:

The aligned lipid bilayers of MPS, MPS with incorporated LPS (3, 5, 7 and 10 wt%), and in the presence of 4 wt% of PxB, respectively, were hydrated with 4 different contrast D_2O/H_2O mixtures. The humidity of 97% was established by the saturated aqueous solution of K_2SO_4 in a small container placed at the bottom of the humidity chamber. The temperature within the chamber was maintained at 45 ^oC to secure the liquid-crystalline state of the lipid. This setup allowed us to attain a stable condition for the sample hydration. Fig. 3a shows repeat distances of MPS+LPS lamellae as a function of the LPS content hydrated with individual D_2O/H_2O contrasts and measured independently. Data were derived from diffraction patterns using Mantid software. Repeat distance *d* increases with the LPS content (shown also in Fig.1b). The scatter of repeat distances, $\Delta d=|d_{max}-d_{min}|\leq 0.6$ Å, taking maximal and minimal value of *d* gained for the sample at different contrasts, except the sample MPS+10 %LPS in 100 % D_2O where care must be taken in the next analysis. The surface of MPS is negatively charged due to the POPG fraction; thus, the stability of the sample during the measurements plays a key role for the next analysis. These results indicate a stable system, allowing data to be combined for analysis [7] to extract the water distribution from the NSLD profiles.

Fig 3b shows the average values of *d* as a function of LPS content, and in the presence of 4 wt% by weight of PxB from the measurements of samples in four contrasts. The nominal charge of the PxB molecule is +5. The repeat distance decreases because of the electrostatic attraction between MPS mediated by cationic PxB. The finding is consistent with our previous results [1,2]. Thus, the obtained data provide both scattering amplitudes and their phases, allowing Fourier transform analysis [4] and the construction of NSLD profiles. The adaptation of Mantis software to extract the diffraction curve from the SAND pattern is in progress. The experimental findings obtained under the MPS-LPS-PxB project were presented in 2022 on [7].

Fig. 3a Repeat distances of MPS+LPS as a function of the LPS content derived from the SAND patterns of samples hydrated with various D_2O/H_2O mixtures. b) Average repeat distance *d* of the MPS+LPS system and the effect of 4 wt% PxB. The error bars are the result of the scatter of *d* values obtained for 4 contrasts.

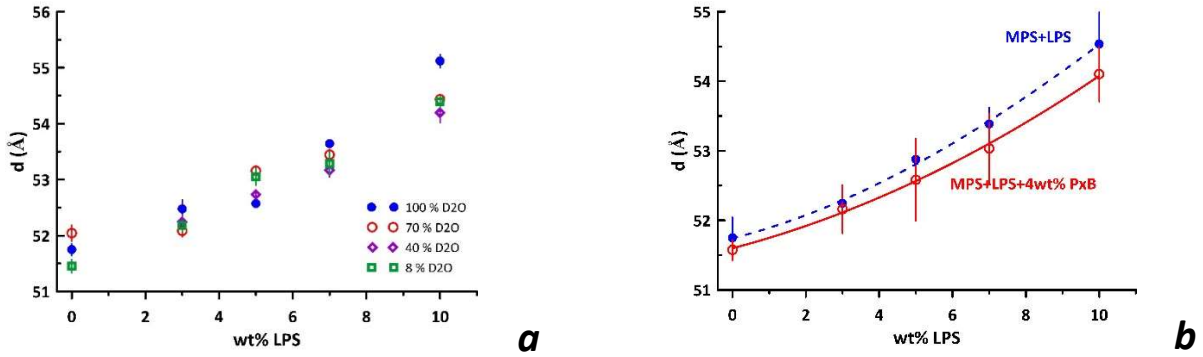

Acknowledgment.: D.U., N.K. and L.H. thank ILL for hospitality. The experiments were supported by VEGA 1/0223/20.

References:

[1] Kolomaznik M., Liskayová G., Kanjaková N., Hubčík L., Uhríková D., Čalkovská A.: *Int. J. Mol. Sci* 19 (2018) 1964
[2] Uhríková D., Kučerka N., Kanjaková N., Demé B.: *ILL experimental report 8-02-927*, 2021
[3] Čalkovská A., Haegerstrnad-Bjorkman M, Curstedt T.: *Sci Reports* 11 (2021) 22
[4] Harroun T.A., Katsaras J., Wassall S.R.: Biochemistry 47 (2008) 7090–7096;
Kučerka N., Ermakova E., Dushanov E., Kholmurodov K.T., Kurakin S, Želinská K, Uhríková D.: *Langmuir* 37 (2021) 278-288
[5] D'Ericco G., Silipo A., Mangiapia G., Molinaro A., Paduano L., Lanzetta R.: *Phys. Chem. Chem. Phys* 11 (2009) 2314-2322
[6] MANTID: O. Arnold, et al., Mantid—Data analysis and visualization package for neutron scattering and μSR experiments, Nuclear Instruments and Methods in Physics Research Section A, 764 (2014)156-166
[7] Uhríková D, Hubčík L, Královič N, Kučerka N, Čalkovská A: 14th International Conference on Physics of Advanced Materials (ICPAM-14), Dubrovnik, Croatia, September 2022, Book of Abstracts, p. 77-79 (invited)
Uhríková D, Královič N, Hubčík L, Kučerka N, Demé B, Combet S, Teixeira J: International meeting on challenges and opportunities for HICANS (IMOH22), Bilbao, June 2022, Book of Abstracts, p. 22 (oral)